Review

Seawater Extractable Organic Matter (SWEOM) Derived from a Compost Sample and Its Effect on the Serving Bioavailable Fe to the Brown Macroalga, *Saccahrina japonica*.

Hisanori Iwai[1*], Masami Fukushima[2], Mitsuo Yamamoto[3], and Taizo Motomura[4]

1 Graduate School of Engineering, Osaka Prefecture University, Sakai 599-8531, Japan
2 Graduate School of Engineering, Hokkaido University, Sapporo 060-8628, Japan
3 Ocean Alliance, The University of Tokyo, Kashiwa 277-8564, Japan
4 Muroran Marine Station, Field Science Center for Northern Biosphere, Hokkaido University, Muroran 051-0013, Japan

Abstract

Barren ground, which is phenomenon associated with the depletion of seaweed beds in coastal areas, is a serious problem for coastal ecosystems and the fishery industry. The lack of dissolved iron is thought to be a major contributing factor for this phenomenon. Because iron species are only slightly soluble in oxic and weak alkaline aqueous around pH 8 like seawater, dissolved organic matter can serve as a chelator to stabilize dissolved Fe species. Based on this background, Fe-fertilizers including steelmaking slag and compost could be used to increase the supply of dissolved Fe species along barren coastlines. Although humic substances in compost would be expected to function as a chelator of Fe, they are flocculated in seawater. We have examined a seawater extractable organic matter (SWEOM) in compost as a novel chelator for use in applications to seawater. In this review, recent studies of the structural features of SWEOM and its complexation with iron are discussed. The roles of SWEOM in the bioavailability of Fe are also discussed, based on the evaluation of gametogenesis in the brown alga, *Saccharina japonica*.

Keywords: SWEOM, Complexation, Bioavailability, Iron, Seaweed, Restoration

Introduction

Seaweed-beds play an important role in the protection of ecosystems and carbon fixation in coastal areas. It has been estimated that the potential biomass productivity for a macro algal forest is 1 – 3.4 kg-C m^{-2} $year^{-1}$, which is two times higher than those of tree plantations or grasslands in temperate regions (Gao and McKinley, 1994; Chung et al., 2011). In Japan, edible seaweeds, especially “Kombu”, “Nori” and “Wakame”, have been important food products for a long time. Recently, seaweed depletion has become a conspicuous worldwide phenomenon (e.g., Millar, 2003; Graham, 2010), which can be attributed to land reclamation, shore protection, tidal flats and other human impact. Apart from this type of seaweed-depletion, barren ground of coastal areas has also been recognized as “*Isoyake*”, which has been a serious coastal problem in Japan since the 1800s (Fujita, 2010).

A variety of reasons for the depletion of seaweeds have been reported: e.g., an increase in water temperature (Tegner and Dayton, 1991), grazing by sea urchins (Fujita, 2010; Tegner and Dayton, 1991; Abraham, 2007), and oligotrophic nutrition (Matsunaga et al., 1994). Recently, the lack of dissolved iron related to the inhibition of iron input from the rivers due to suburban development, such as the construction of dams and embankment works (Matsunaga et al., 1999). Matsunaga et al. (1994) reported that the iron concentration in the barren coast of the Japan Sea was less than 2 nM, and biomass productivity for a brown macroalga (*Saccharina japonica*) was significantly increased

* Corresponding author: Tel. +81-72-254-7254, E-mail h-iwai@marine.osakafu-u.ac.jp

when higher levels (10 – 50 nM) of dissolved iron were present (Matsunaga et al., 1994). The impact of grazing by sea urchin can be estimated from the relationship between grazing and biomass productivity for seaweed (Abraham, 2007; Perreault et al., 2014). Under the lower level of dissolved iron, the resistance of seaweeds to grazing by herbivores would be significantly decreased, and this leads to the development of a barren coast. Therefore, a high level of dissolved Fe is required in order to preserve seaweed-beds where herbivorous animals are present. In addition, it is known that iron is essential for inducing gametogenesis of brown macroalgae (*S. japonica, S. angstata and Desmarestia ligulata*) (Motomura and Sakai, 1981; Motomura and Sakai, 1984). As shown in Fig. 1, sporophytes, which are a macroscopic life stage for laminarialean algae, are formed from fertilized eggs (Lobban and Harrison, 2000). For these reasons, increasing the levels of dissolved iron is one of the important factors in restoring seaweed beds in coastal areas. However, iron species are only slightly soluble in seawater under oxic (E_h = 0 – 50 mV) and weak alkaline conditions (pH 7.8 – 8.1), because iron immediately precipitates as colloidal forms, such as hydroxides. It has been reported that the majority of dissolved iron in seawater is present as in complexed form with dissolved organic matter (DOM) (Macrellis et al., 2001; Laglera and van den Berg, 2009). By definition, DOM includes both humic substances (HSs) and non-HSs (e.g., amino acids, peptides, proteins, saccharides and polysaccharides) (Tan, 2003a). Compost is expected as a source of DOM because it is rich in HSs and non-HSs. Based on such a concept, the restoration of seaweed beds using an Fe-fertilizer composed of steelmaking slag and compost as sources of iron and DOM, respectively, were examined (Yamamoto et al., 2010a). This technique was found to be effective in increasing iron concentration and restoring of seaweed beds in barren coastal areas (Yamamoto et al., 2010a). However, little is known regarding the effects of DOM derived from the Fe-fertilizer on iron species and their bioavailability to brown macroalgae.

It has been well known that among the DOM, humic (HA) and fulvic (FA) acids can serve as major chelators for binding various metal cations (Tipping, 2002a). These functions for DOM can play an important role in determining the water solubility, mobility, speciation and bioavailability of trace metals in an aquatic environment (Tipping, 2002b). In the restoration technique, the elution of iron from steelmaking slag and the stabilization of the eluted iron were enhanced by mixing with a compost

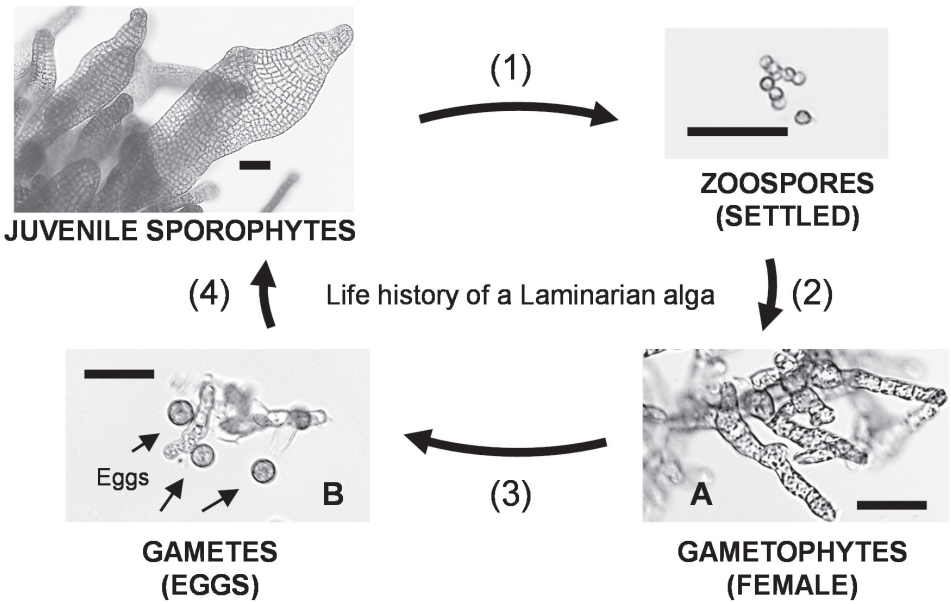

Figure 1. Life history of laminarialean algae. (1) Juvenile sporophytes grow to adult sporophytes (macroscopic), and produce unilocular sporangia. Zoospores are released from them. (2) Zoospores develop into male or female gametophytes. (3) Gametophytes become matured, and release gametes (eggs and sperm). (4) Fertilized eggs can grow into juvenile sporophytes. Photograph A and B represent the female gametophytes and eggs, respectively. Scale bars indicate 50 μm.

(Yamamoto et al., 2012). This result indicates that compost plays a key role in increasing dissolved iron in seawater. Because HSs are considered to be a representative fraction of DOM, HSs have been employed in many investigations of the role of DOM in the environment (e.g., Fujii et al., 2014; Ytreberg et al., 2011; Fukushima et al., 1999). To understand the roles of compost in Fe-fertilizer for restoration, previous studies have focused on the role of HS fractions, such as the binding characteristics of Fe(II), the contribution to Fe elution rate and structural alterations in HSs (Yamamoto et al., 2010b; Yamamoto et al., 2012; Fujisawa et al., 2012). For a better understanding of the role of HSs in supplying dissolved Fe in a bioavailable form to seaweeds, the behavior of HSs under seawater conditions need to be investigated. However, HSs are easily aggregated under conditions of higher concentrations of multivalent cations, such as Ca^{2+} and Mg^{2+}, as are found in seawater (Tipping, 2002c). As shown in Fig. 2, HA and FA derived from a compost were easily aggregated and precipitated by adding artificial seawater (Fukushima and Iwai, 2011). HA and FA are fractions defined by the extraction procedures used in their isolation, that is, their solubility in base and acid, and their adsorptivity to DAX-8 resin (Tan, 2003b; Tipping, 2002d; Swift, 1996). These extracting conditions (pH 11 – 12) were far from that for seawater (pH 7.8 – 8.0). The nature of the DOM derived from a compost can be regarded as a key factor for understanding the mechanical aspects of the restoration technique, however, it may be different from those of HSs. This leads to the suggestion that not HSs, but, rather, the DOM fraction extracted under actual conditions can serve as a chelator of iron in seawater. Thus, our research group focused on a novel fraction, seawater extractable organic matter (SWEOM), in the compost sample.

In this paper, a series of studies on SWEOM, which includes the structural features, binding abilities to Fe(II), are reviewed. In addition, the efficiency of Fe and SWEOM on reproductive growth in the brown alga, *S. japonica*, and insights in iron uptake mechanism were described. Significance of the obtained results was discussed to apply to restoration of seaweed bed in the barren coast.

Structural features of SWEOM

The SWEOM is a novel DOM fraction from compost sample. First, to better understand the characteristics of the SWEOM, its structural features were investigated by comparing with those of HA and FA from a compost sample (Iwai et al., 2013a; Iwai et al., 2013b).

Extraction and purification methods of SWEOM

A bark compost (Tokachi bark, FOREX, Hokkaido) was employed for the preparation of the SWEOM and HSs. A mixture of dry compost and artificial

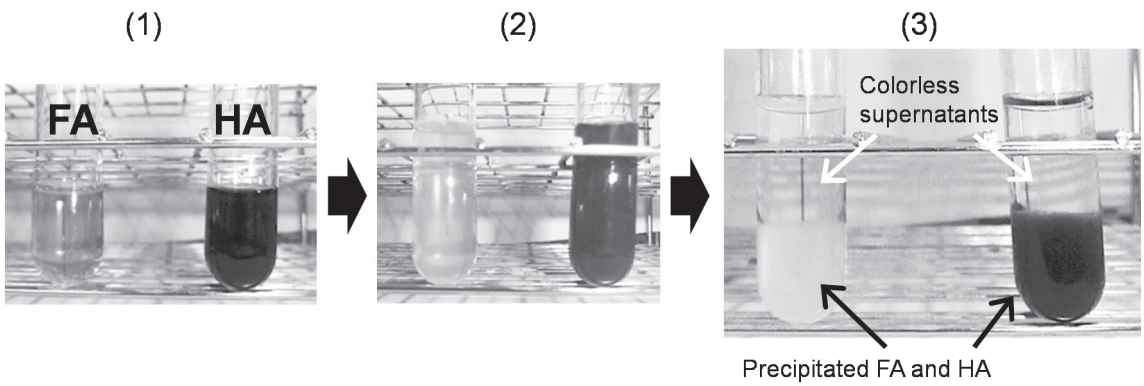

Figure 2. Coagulation of FA (left) and HA (right) derived from a bark compost in seawater. (1) Before adding seawater, the color of HA and FA solutions (5 mL, 1000 mg mL^{-1} in 0.05 M NaOH) were dark brown and yellow, respectively. (2) After adding artificial seawater (pH 8.1), these solutions were suspended immediately. (3) After standing for a half-day, the flocculated HSs had precipitated (black arrows in (3)) and the supernatants were colorless (white arrows in (3)). These pictures were referred from Fukushima and Iwai (2011), *J. Adv. Mar. Sci. Technol. Soc*., © Advanced Marine Science and Technology Society 2014.

seawater at pH 8.1 (Solid/Liquid = 1/10, w/w) was shaken under a N_2 atmosphere and in the dark for 3 days. After the centrifugation of the mixture, the supernatant was filtered through a 5A filter, and the filtrate was fractionated by means of an ultrafiltration membrane filter with a nominal molecular weight cut-off of 500 Da (Millipore). A molecular weight fraction above 500 Da (MWA) was deionized by washing with ultrapure water and then dialyzed using Spectra/Por dialysis membrane (molecular weight cut-off of 500 Da) against ultrapure water. The molecular weight fraction below 500 Da (MWB) was acidified to pH 1 – 2 and adsorbed to DAX-8 resin. Subsequently, the adsorbed MWB was eluted with aqueous 0.01 M NaOH, and the eluate was then passed through a H^+-type cation exchange resin column. More detailed procedure of the method has been described in previous reports (Iwai et al., 2013a; Iwai et al., 2013b). FA and HA were extracted and purified in accordance with a method approved by the International Humic Substances Society (e.g., Fukushima et al., 2006; Swift, 1996). The powdered form of the samples was obtained by freeze-drying and then analyzed.

Structural affinities of SWEOM

The yields, elemental compositions, atomic ratios, total amino acid and acidic functional group contents of the product are summarized in Table 1. The O/C atomic ratios for SWEOM samples were comparable to that for FA, suggesting that SWEOMs contain a large amount of oxygen-containing functional groups. The contents of acidic functional groups (carboxylic acids and phenolic hydroxyl groups) for MWB were much higher than those for MWA, and similar to those for FA. In addition, the acidic functional group contents for MWA were smaller than those for HSs. These results show that the larger level of O/C ratio in MWA can be attributed to ether and ester moieties. The H/C and N/C atomic ratios for the MWA were larger than those for MWB and HSs, suggesting that MWA is composed of higher amounts of saturated hydrocarbons and nitrogen-containing compounds, such as peptides and proteins.

Figure 3 shows FT-IR spectra of the SWEOMs and HSs samples. The peaks at 2850 – 2950 cm^{-1} for MWA, which indicate asymmetric and symmetric stretching of methyl and methylene C-H bonding, were larger than those for HSs. The large peaks at around 1050 cm^{-1} for MWA were assigned to C-O-C stretching of ethers or C-O stretching for aliphatic alcohols. The bands at 1550 and 1650 cm^{-1} for MWA can be assigned as amide-I and -II bands, respectively. These data indicate that MWA includes higher levels of aliphatic alcohols, peptides and proteins, consistent with the elemental analysis results (Table 1). The shape of FT-IR spectrum for MWB was similar to that for FA. These spectra show a large peak at around 1720 cm^{-1}, which can be

Table 1 Yields, elemental compositions, atomic ratios, total amino acid and acidic functional group contents for SWEOM (MWA and MWB), FA and HA (Iwai et al., 2013a and 2013b).

		SWEOM			
		MWA	MWB	HA	FA
Yields (g kg^{-1})$^{\alpha}$		1.20	1.30	58.0	1.90
Elemental composition (%)	C	45.7	46.1	51.9	45.3
	H	6.27	4.74	5.26	4.5
	N	6.41	4.07	5.11	3.85
	O	38.1	38.1	28.8	41.6
	S	0.84	1.36	8.54	1.69
	Ash	2.74	6.04	0.41	3.06
Atomic ratio	H/C	1.64	1.22	1.21	1.18
	N/C	0.12	0.08	0.08	0.07
	O/C	0.63	0.62	0.42	0.69
Total amino acid content (mg g^{-1}-Sample)		153	28.2	62.3	16.9
Acidic functional group content (mmol g^{-1}C)	-COOH	3.85	11.5	4.8	15.5
	Phenolic-OH	3.75	8.09	5.9	3.64

$^{\alpha}$ Yields were calculated as final amount of dried powdered sample (g) in a dried bark compost taken for the extraction initially (kg).

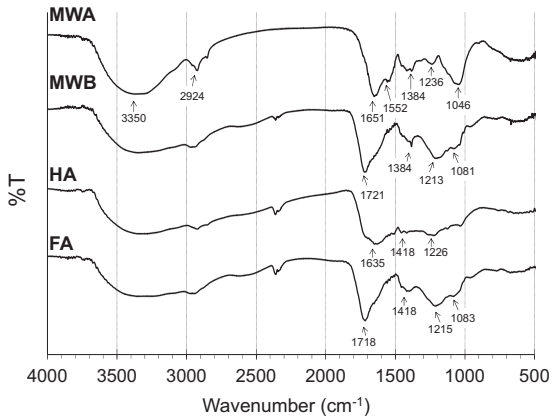

Figure 3. FT-IR spectra for SWEOMs and HSs with a KBr disk (Iwai et al., 2013a; Iwai et al., 2013b). Assignments of the spectral bands were referred to Silverstein and Webster (1998).

assigned as C=O stretching of carboxylic acid, consistent with the higher levels of carboxylic acids (Table 1).

Figure 4 shows solid-state CP-MAS ^{13}C NMR spectra for SWEOM and HS samples. The MWA contains higher levels of aliphatic alcohols and ethers (60 – 90 ppm) (ca. 29%). The peaks appearing above 105 ppm for MWA (ca. 31%) were smaller than those for the MWB (ca. 47%) and HSs (ca. 55% and 54% for HA and FA, respectively). The peaks appearing at 105 – 160 ppm and 160 – 180 ppm can be assigned as aromatic and carbonyl (acids, esters and amides) carbons, respectively. For MWB, the peaks corresponding to aromatic and carbonyl carbons were more intense than those for MWA. These results are consistent with the trends in atomic ratios, which are the higher H/C and lower O/C ratios in MWA and the lower H/C and higher O/C ratios in MWB.

The sub-units of MWA and HSs were compared by pyrolysis-GC/MS (py-GC/MS) with tetramethylammonium hydroxide (TMAH). The relative peak areas of classified pyrolysate compounds in MWA and HSs are summarized in Table 2. The levels of fatty acids and sterol pyrolysate compounds, which are derived from plant wax and microbial origin, for MWA were significantly higher than those for HSs (Table 2). As shown in Table 1, the carboxylic acid and phenolic hydroxyl group contents for the MWA were significantly lower than those for HSs. In addition, phosphoric acid trimethyl ester, derived from the

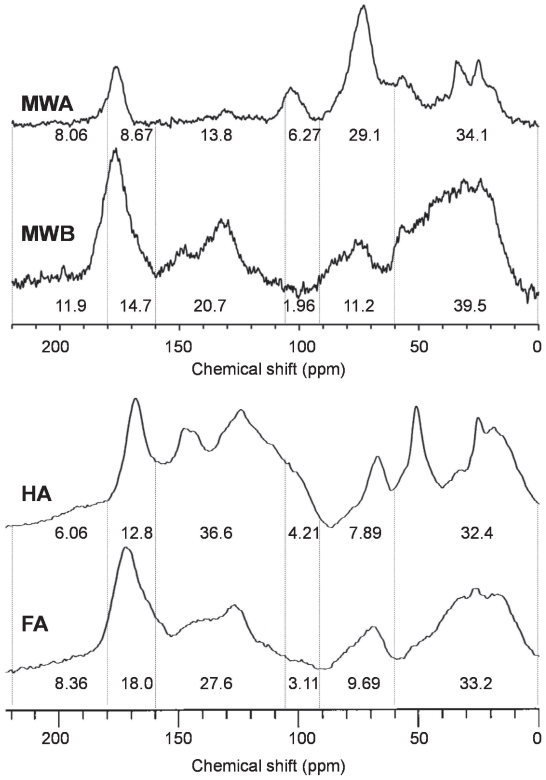

Figure 4. Solid-state CP-MAS ^{13}C NMR spectra for SWEOMs and HSs. The labeled values under spectra indicate the compositions (%) of carbon species for each area corresponding to the following assignments: 0 – 60 ppm is alkyl carbons; 60 – 90 ppm is aliphatic alcohols and ethers carbons; 90 – 105 ppm is anomeric carbons; 105 – 160 ppm is aromatic carbons; 160 – 180 ppm is carbonyl carbons (acids, esters and amides); 180 – 220 ppm is carbonyl carbons (quinones, ketones and aldehydes) (Iwai et al., 2013a; Iwai et al., 2013b). Assignments of the peaks were referred to Warshaw et al., (1998).

cleavage of phospholipids, was detected only in the MWA (Iwai et al., 2013a). Thus, the majority of fatty acids in MWA are present as the form of esters, and some of fatty acids in the MWA were derived from the cleavage in ester-linkages of phospholipids caused by the pyrolysis. The nitrogen-containing pyrolysate compounds in Table 2 are likely derived from amino acids, peptides, proteins and nucleic acids. However, the relative peak areas were not correlated with the trends in the N/C ratio and the peak intensities for the peptide band in the FT-IR spectra. Methylindole was detected as a major pyrolysate compound (22 and 60 % of the nitrogen-containing compounds for MWA and HA, respectively). This compound is formed by the

Table 2 Relative areas of pyrolysate compounds detected in MWA, HA and FA (Iwai et al., 2013a).

Classification	Relative peak areas[α]		
	SWEOM (MWA)	HA	FA
Furan derivatives	n.d.[β]	n.d.[β]	32.0
Nitrogen-containing compounds	193	119	367
Methoxy- and Hydroxy- benzenes	253	582	15.7
Aromatic ketones and aldehydes	n.d.[β]	116	42.6
Phenolic and Aromatic acid	158	343	24.8
Saturated fatty acids	1034	128	226
Unsaturated fatty acid	377	25.7	256
Sterols	143	16.7	5.89
Terpenoids	30.1	27.5	21.5
Others	49.8	23.3	17.4

[α] Values for each pyrolysate compounds groups represent percent of relative area to internal standard. Nonadecanoic acid, 10 μL of 0.06 mg mL^{-1} was added to 1 mg samples for the internal standard.
[β] Not detected.

pyrolysis of tryptophan (Gallois et al., 2007). Indole is a representative example of pyrolysate compounds derived from amino acids (Gallois et al., 2007), while this cannot be used for the quantitative analysis of amino acids.

Some reports have focused on water-extractable organic matter (WEOM) for assessing the maturity of the compost (Said-Pullicino et al., 2007; He et al., 2011; Lv et al., 2013). These reports showed that, in a WEOM derived from a mature compost, aliphatic materials, carbohydrates and nitrogen containing compounds have been lost, and the materials is enriched in carboxyl groups and aromatic compounds (Said-Pullicino et al., 2007; He et al., 2011; Lv et al., 2013). However, these features differ from that of SWEOM, except that the hydrophobic fraction in WEOM is similar to that for the MWB (Said-Pullicino et al., 2007).

These results showed the uniqueness of SWEOM as the DOM fraction from compost. In the SWEOM fraction, a distinction between the molecular weight fractions above (MWA) and below (MWB) 500 Da can be made based on their structural features. The SWEOM contained a higher level of oxygen, while, the acidic functional group content for MWA was lower than that for HS. MWA contained a higher level of nitrogen-containing compounds, lipids and saturated hydrocarbons. MWB contained the large amounts of acidic functional groups, a characteristic that is similar to FA.

Binding abilities to Fe(II) under seawater conditions

Iron can be eluted from Fe(III)-oxides in steelmaking slag, such as magnetite and hematite (Nishimoto et al., 2013), as a ferrous form under seawater conditions, which may occur as the result of reduction by humic substances or metabolites of bacteria (Fujisawa et al., 2012; Nishimoto et al., 2013). However, ferric species are readily precipitated in the form of hydroxides (Pham et al., 2006). SWEOM would be expected to serve as a chelator of the eluted Fe(II), and may contribute to the stabilization of dissolved species of iron in seawater. An evaluation of the binding abilities to Fe(II) is needed to better understand the function of SWEOM in a compost. Thus, the binding constants, capacities and dissociation kinetics constants for Fe(II) complexes with SWEOM or HSs were evaluated (Yamamoto et al., 2010b; Fujisawa et al., 2011; Iwai et al., 2012). Alginic acid and fucoidan, which are constituents of brown algal cell wall, adsorbed divalent metals (Manley and North, 1981). Paskins-Hurlburt et al. (1978) showed that fucoidan from *Ascophyllum nodosum* has a high affinity for Fe^{2+} as compared with most of the other divalent metals (Paskins-Hurlburt et al., 1978; Manley, 1981). Based no this, it can be considered that the transfer of Fe complexed with DOM to the binding sites is a primary reaction for iron uptake. Iwai et al. (2012)

investigated the transfer of iron from Fe(II)-SWEOM complexes to the strong chelator, *ortho*-phenantroline (OP). The entropy for the dissociation of the activated complex ($\Delta S^{\ddagger}$) for Fe(II)-SWEOM and Fe(II)-HSs were negative (ca. −250 J K^{-1} mol^{-1}), indicating that the reaction intermediate for the dissociation of Fe(II)-DOM complex *via* a ligand-exchange with OP is the ternary complex, OP-Fe(II)-DOM. From this result, it would be expected that the strong binding sites on the cell membrane might not necessarily proceed *via* free Fe species dissociated from DOM but, rather, by a ligand-exchange reaction involving the ternary complex as an intermediate. In addition, the energy for dissociation of the activated complex ($\Delta H^{\ddagger}$) for Fe(II)-SWEOM complex ($\Delta H^{\ddagger}$ = 19 kJ mol^{-1}) was significantly smaller than the corresponding values for Fe(II)-HSs complexes ($\Delta H^{\ddagger}$ = 25 − 30 kJ mol^{-1}), suggesting that Fe(II)-SWEOM complex is more exchangeable and bioavailable than those with HSs (Iwai et al., 2012). From these findings, labile Fe(II) species complexed with DOM can be expected to be the bioavailable species. However, these experimental conditions (pH 3.6 or 5, I = 0.02) employed in the study by Yamamoto et al. (2010b), Fujisawa et al. (2011) and Iwai et al. (2012) were far from those for seawater (pH 8, I = 0.7). Indeed, pH, ionic conditions and the presence of competitive cations can effect on the speciation of dissolved metal ions and the nature of DOM (Rosen, 1978; Mathuthu and Ephraim, 1993; Fukushima et al., 1994; Fukushima et al., 1995). To better understand the performance of the SWEOM, the binding abilities should be evaluated under seawater condition. Thus, an analytical technique for evaluating the binding abilities to Fe(II) under seawater conditions (pH 8, I = 0.7) is described in the following subsections (Iwai et al., 2013b).

Determination of labile complex Fe(II) species

The labile species of Fe(II)-SWEOM complexes were determined by the measurement of colored Fe(II)-ferrozine (FZ) complex formation *via* a ligand-exchange reaction between SWEOM and FZ. In order to preserve Fe(II), an artificial seawater containing ascorbic acid as an antioxidant was prepared, as summarized in Table 3. In the presence of SWEOM, the colored Fe(II)-FZ complex is formed by the following two reactions:

Table 3 Compositions (g L^{-1}) of the artificial seawater buffer (pH 8.0$^{\alpha}$).

NaCl	28.0
KCl	0.70
$MgSO_4 \cdot 7H_2O$	7.00
$MgCl_2 \cdot 6H_2O$	4.00
$CaCl_2$	1.11
Tris$^{\beta}$	1.20
Ascorbic acid$^{\gamma}$	1.76

$^{\alpha}$ pH was adjusted after added of ascorbic acid.
$^{\beta}$ Tris(hydroxymethyl)amminomethane.
$^{\gamma}$ Ascorbic acid was added to the buffer immediately prior to use.

$$Fe^{2+} + FZ \rightleftharpoons Fe(II)\text{-}FZ \quad (1)$$

$$Fe(II)\text{-}SWEOM_{labile} + FZ \rightleftharpoons SWEOM + Fe(II)\text{-}FZ \quad (2)$$

where Fe^{2+} and $Fe(II)\text{-}SWEOM_{labile}$ represent free species of Fe^{2+} and labile species of Fe(II)-SWEOM complexes, respectively. In the mixture of Fe^{2+} and SWEOM, free species of Fe^{2+} can rapidly be colored by complexation with FZ. The kinetics of the formation of Fe(II)-FZ in the absence and presence (50 mg L^{-1}) of SWEOM (MWB) was investigated by means of a stopped-flow spectrophotometry (Fig. 5) (Iwai et al., 2013b). A fast reaction between free species of Fe^{2+} and FZ was detected for 0.03-s (meshed region in Fig. 5 A). This fast increasing of Fe(II)-FZ was also occurred in the reaction between FZ and the mixture of Fe(II) and SWEOM (meshed region in Fig. 5 C). After 0.03-s in Fig. 5 C, steadily increasing of Fe(II)-FZ, which can be attributed to the ligand-exchange reaction in Eq. 2, was detected. The formation of Fe(II)-FZ was not detected in the reaction between SWEOM and FZ (Fig. 5 B). Thus, labile species of Fe(II)-SWEOM complexes can be determined based on the kinetics of the coloration of Fe(II)-FZ. Figure 6 shows the kinetic curves for the formation of the colored Fe(II)-FZ complex based on Eqs. 1 and 2 measured by means of UV-vis spectrophotometer. As shown in Fig. 6, the absorbance up to a 3-s reaction period was considered to be the complexation reaction between free species of Fe(II) and FZ by Eq. 1. After the 3-s reaction period, the colored Fe(II)-FZ is formed via a ligand-exchange reaction, as shown in Eq. 2. The end point of the reaction is indicated by a point, at which the variation in the absorbance for a 10-s interval was within ± 0.001. The concentration of labile Fe(II)

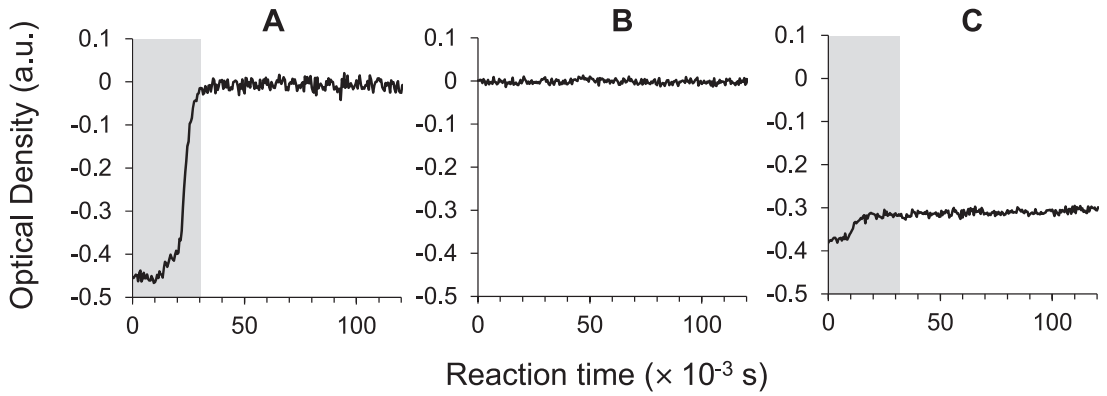

Figure 5. The kinetic curves for the formation of Fe(II)-FZ complex in the absence (A) and presence (B and C) of SWEOM under an artificial seawater buffer (pH 8.0, I = 0.7, [Ascorbic acid] = 10 mM) collected using an RSP-1000-02 type stopped-flow spectroscopy system (UNISOKU, Co. Ltd.). These curves for A, B and C were derived from reactions of FZ + Fe^{2+}, SWEOM + FZ and Fe(II)-SWEOM + FZ, respectively. The initial concentration of Fe(II) for A and C were prepared to 30 μM. The concentration of SWEOM (MWB) for B and C were prepared to 50 mg L^{-1} (Iwai et al., 2013b).

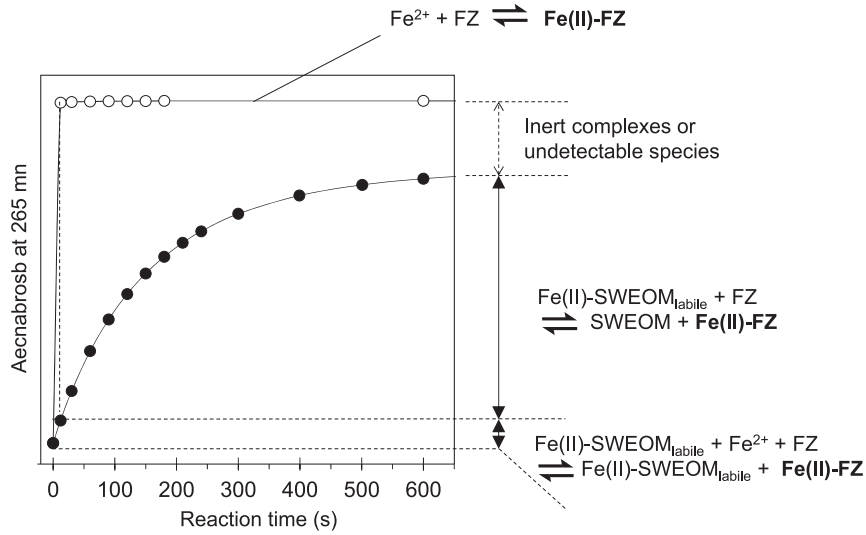

Figure 6. Kinetics of the increase in absorbance at 562 nm by forming Fe(II)-FZ in an artificial seawater buffer (pH 8.0) (Table 3). Open circles indicate the binding kinetics of FZ to Fe^{2+}. Closed circles indicate kinetics of a ligand-exchange reaction between Fe(II)-$SWEOM_{labile}$ and FZ ([SWEOM] = 50 mg L^{-1}). The coloration that increased rapidly within several second in the closed circles can be regarded as the binding reaction between FZ and free Fe^{2+}. The total concentrations of Fe were 10 μM (Iwai et al., 2013b).

species complexed with SWEOM was calculated from the absorbance at this region, as shown in Fig. 6.

Evaluation of complexing abilities of SWEOM to Fe(II)

Assuming a 1:1 molar ratio for complexation between Fe(II) and an arbitrary binding site in SWEOM (Iwai et al., 2012), the conditional binding constant (K_b) and total concentration of binding sited (C_L) for labile Fe(II)-SWEOM complexes can be written as follows:

$$K_b = \frac{[\text{Fe(II)-SWEOM}]_{\text{labile}}}{[\text{Fe(II)}]_{\text{free}}\,[\text{SWEOM}]} \quad (3),$$

$$C_L = [\text{SWEOM}] + [\text{Fe(II)-SWEOM}]_{\text{labile}} \quad (4),$$

where [SWEOM] and $[\text{Fe(II)-SWEOM}]_{\text{labile}}$ represent the concentrations of SWEOM and labile Fe(II)-SWEOM complexes, respectively. The relationship between the concentrations of free Fe(II) ($[\text{Fe(II)}]_{\text{free}}$) and labile Fe(II)-SWEOM complexes can be derived

by combining Eqs. 3 and 4:

$$[\text{Fe(II)-SWEOM}]_{\text{labile}} = \frac{K_b \times C_L \times [\text{Fe(II)}]_{\text{free}}}{1 + K_b\,[\text{Fe(II)}]_{\text{free}}} \quad (5).$$

K_b and C_L were calculated by the non-linear least square regression analysis of data set for $[\text{Fe(II)}]_{\text{free}}$ and $[\text{Fe(II)-SWEOM}]_{\text{labile}}$ to Eq. 5. The binding capacity can also be calculated as shown below:

$$\text{Binding capacity (molg}^{-1}\text{ C)} = \frac{C_L}{[\text{SWEOM}]\,(\text{gL}^{-1}) \times \%C} \times 100 \quad (6).$$

where the concentration of the SWEOM was set at 0.05 g L^{-1}, and the %C value in Table 1 was employed. Figure 7 shows the relationships between $[\text{Fe(II)}]_{\text{free}}$ and $[\text{Fe(II)-SWEOM}]_{\text{labile}}$. The experimental data sets were well fitted to Eq. 5 ($R^2 > 0.98$). The values for logK_b and binding capacities for MWA and MWB, calculated from the curve-fitting, are summarized in Table 4. The logK_b for MWA was slightly higher than that for MWB. The value of the binding capacity for the MWB was significantly larger than that for MWA, consistent with the higher levels of acidic functional groups in the MWB (Table 3). Because Fe(II) is classified as a borderline acid based on the HSBA principle, nitrogen-containing groups like amines of borderline base are favorable ligands for Fe(II) (Perdue et al., 1976). Thus, the higher level of nitrogen in the MWA contributes to the higher value of logK_b. However, it is known that carboxylic acids and phenolic hydroxyl groups serve as the dominant binding sites for DOM and HSs. For SWEOM, the levels of oxygen-containing groups are much larger than nitrogen-containing groups (O/C and N/C ratio in Table 1). Compared with the binding abilities for the corresponding values in Iwai et al. (2012) and Iwai et al. (2013b), although in the presence of competitive divalent cations, such as Ca^{2+} and Mg^{2+}, the binding capacity of MWA under the seawater conditions was significantly larger than that in acetate buffer (Table 4) (Iwai et al., 2012; Iwai et al., 2013b). Because the competition of H^+ with the metal for the ligand decreases, the amounts of bound metal ions increase at higher pH values (Tipping, 2002c). In addition, under high ionic strength conditions, the surface negative charges can be enlarged, probably a result of conformational changes caused by the neutralization of the repulsions caused anionic charges in their structure (Rosen, 1978; Fukushima et al., 1994). These trends would be predicted to increase the binding capacity, and indicate that the acidic functional groups in SWEOM can serve as binding sites for Fe(II). Thus, SWEOM can function as a chelator of Fe in seawater.

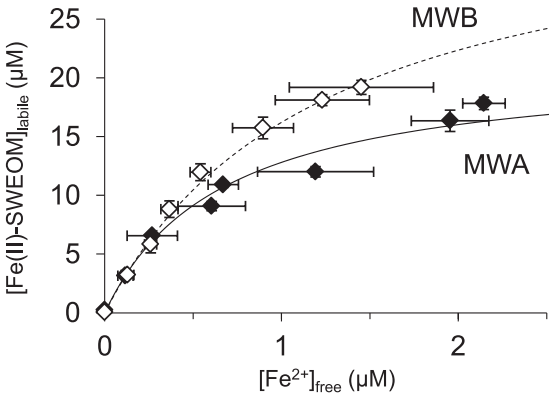

Figure 7. Relationship between Fe(II) and Fe(II)-SWEOM concentrations at 50 mg L^{-1} of SWEOM: plots and error bars represent average values of MWA (filled diamonds) or MWB (open diamonds) and standard deviations ($n = 4 - 5$), respectively. Solid and broken lines represent fitting curves for MWA and MWB, respectively (Iwai et al., 2013b).

Effect of SWEOM on the bioavailability of iron to a brown macroalga

Phycological investigations are needed to clarify the effect of the Fe-fertilizer to the restoration of

Table 4 Conditional binding constants (log K_b) for labile Fe(II)-SWEOM complexes and the binding capacities of SWEOM samples for Fe(II) (Iwai et al., 2012; Iwai et al., 2013b).

	MWA		MWB
logK_b	5.63 ± 0.15	6.17 ± 0.09	5.91 ± 0.12
Binding capacity (μmol g^{-1}C)	80.0 ± 7.9	936 ± 93	1546 ± 215
Buffer (pH)	0.2 M Acetate buffer (3.6)	Artificial seawater buffer (8.0)	Artificial seawater buffer (8.0)
Indicator of Fe(II)	*ortho*-Phenantroline	Ferrozine	Ferrozine
References	Iwai et al. (2012)	Iwai et al. (2013b)	Iwai et al. (2013b)

seaweed-beds. For laminarialean algae, as shown in Fig. 1, the reproductive maturation of gametophytes (A to B in Fig. 1) is essential for the formation of sporophytes (Lobban and Harrison, 2000). The influence of environmental factors, such as light, temperature and nutrients, on the reproductive growth was investigated (Lüning and Neushul, 1978; Lüning 1981; Motomura and Sakai, 1981: Motomura and Sakai, 1984). Motomura and Sakai (1981 and 1984) cleared that maturation of the gametophyte is strongly induced by a high concentration of Fe, especially in egg formation (Motomura and Sakai, 1981; Motomura and Sakai, 1984). Therefore, the maturation of female gametophytes (i.e., egg formation or oogenesis) leads to the direct restoration of seaweed-beds, and can be regarded as an indicator of a bioavailability of Fe.

Methods for cultivation and gametogenesis assay

Female gametophytes of *S. japonica* were employed in this study. The stock of gametophytes, which were vegetatively grown under axenic conditions, was obtained from the Charatsunai, Muroran, Hokkaido. The gametophytes were stock-cultured in 25 glass tubes that contained 10 mL of Fe-free ASP_{12} medium (pH 7.8 – 8.0) (Provasoli, 1963), and they were precultured for more than 6 months at 10°C and a 14-h:10-h of light (ca. 10 μE m^{-2} s^{-1} with cool white fluorescent lights) and dark cycle, as described in previous reports (Motomura and Sakai, 1981; Motomura and Sakai, 1984). For inducing gametogenesis, the culture media were prepared by adding chelating agents (EDTA, nitrilotriacetic acid (NTA), catechol (Cat), protocatechuic acid (PCA), ferrichrome (FC), *N*,*N*'-bis(2-hydroxybenzyl) ethylenediamine-*N*,*N*'-diacetic acid (HBED) and SWEOMs) and Fe^{2+} into Fe- and EDTA-free ASP_{12} (pH 7.8 – 8.0), and a 30 mL aliquots of this solution were then pipetted into 100-mL Erlenmeyer flasks. The resulting media were covered with Al-foil, and sterilized by autoclaving (121°C, 20 min). The gametophytes were inoculated into the cooled media under HEPA conditions, and cultured for 14 days at 10°C under condition of a 14-h:10-h light and dark cycle of 20 – 40 μE m^{-2} s^{-1} with cool white LED lights.

The influence of culturing condition on the reproductive growth has been usually evaluated based on maturity, i.e., the percentage of female gametophytes with released eggs. According to previous studies (Lüning and Neushul, 1978; Lüning 1981; Motomura and Sakai, 1981: Motomura and Sakai, 1984; Nigi et al., 2000), the effect of SWEOM to the bioavailability of Fe were evaluated by the percent of maturity which was determined by random counting of more than 100 gametophytes using an inverted microscope (Iwai et al., 2015). More detailed procedures have been described in a previous report (Iwai et al., 2015).

Effect of SWEOM on oogenesis

The effect of Fe concentration on oogenesis is shown in Fig. 8. In the presence of EDTA, the percentages of maturity at day 14 dramatically increased with increasing of Fe concentration from 0.1 to 1 μM, and reached a plateau at Fe concentrations above 1 μM (filled symbols in Fig. 8). In the presence of EDTA ($[Fe^{2+}]$/[EDTA] = 1/1, mol/mol), approximately 84% of the gametophytes matured at an Fe concentration of 1 μM for a 14-day cultivation period (filled circles in Fig. 9). The maturity did not significantly increase in the presence of 10 μM EDTA and Fe (ca. 87 %), suggesting that 1 μM of Fe is sufficient for inducing gametogenesis (Iwai et al., 2015). However, in the absence of a chelator (open symbols in Fig. 8), the majority of gametophytes failed to mature even in the presence of a higher concentration of Fe (10 μM), where the percentage of maturity was less than 10 % (Iwai et

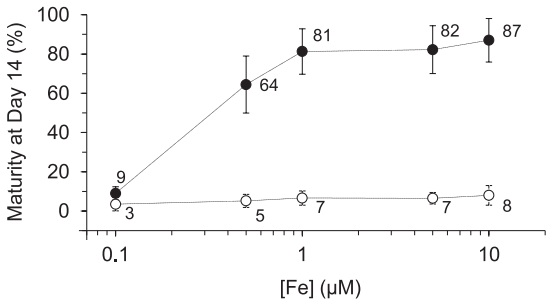

Figure 8. Relationship between the concentration of Fe (μM) and percent maturity (%) for a 14-day incubation period. Filled and open symbols represent the percent maturity in the presence (Fe:EDTA = 1:1 molar ratio) and absence of EDTA, respectively. Plots and labeled values represent average maturity (%), and the error bars represent the standard deviations (n = 4) (Iwai et al., 2015).

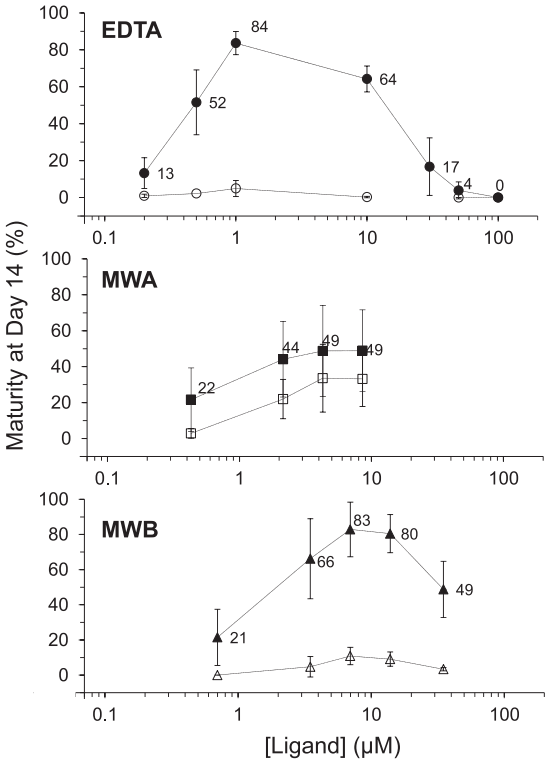

Figure 9. Relationship between ligand concentration (μM) and percent maturity (%) for a 14-day incubation period. Filled and open symbols represent the percent maturity in the presence (1 μM) and absence of Fe, respectively. Circle, square and triangle symbols represent the case of EDTA, MWA and MWB, respectively. For SWEOMs, ligand concentrations were calculated from concentration of SWEOM (mg L^{-1}) and determined values of Fe binding capacities (μmol g^{-1}C) in previous reports (Table 5, Iwai et al., 2013b). Data points and error bars represent the average values and standard deviations (n = 4). Average maturities obtained in the presence of Fe are labeled on the side of filled symbols.

al., 2015). This is because colloidal $Fe(OH)_3$, which is the dominant species in the absence of chelator, is insoluble and therefore unavailable species for inducing maturation (Suzuki et al., 1994). The gametophytes may be possible to slowly take up Fe from colloidal $Fe(OH)_3$ (Suzuki et al., 1995; Nigi et al., 2000), however, as is apparent from this result, complexed Fe species are required for egg formation.

Figure 9 shows the results for the gametogenesis assay for a variety concentration of EDTA and SWEOMs. As shown in Fig. 9, the percent maturities decreased in the presence of an excess concentration of EDTA (10 – 100 μM), compared to that of Fe (1 μM). Only vegetative growth was observed in the case of gametophytes cultured in media containing 100 μM of EDTA, indicating that excess concentrations of chelating agent inhibit the reproductive growth. In the presence of MWA or MWB and 1 μM Fe, 21 – 83 % of the gametophytes reached maturity (Fig. 9). It is noteworthy that a higher maturity (80 %) was observed in the case of MWB, which corresponds to the level in the case of EDTA. A higher concentration of MWA ([Ligand] = 4.28 and 8.56 μM) resulted in the MWA being flocculated during the incubation. This was substantial in the presence of Fe (1 μM), suggesting that flocculation leads to the precipitation of Fe and inhibits inducing gametogenesis. MWB did not precipitate even at a in the higher concentration ([Ligand] = 13.9 and 34.9 μM), although, a higher MWB concentrations above 10 μM the maturities decreased (Fig. 9). This may be due to the presence of excess ligand, as shown in the case of EDTA (Iwai et al., 2015). In the case of MWA alone (open squares in Fig. 9), 4 – 30 % of the gametophytes was converted into eggs. The 18 and 8 μmol g^{-1} of Fe were detected in MWA and MWB samples, respectively (Iwai et al., 2013b). Thus, such the maturation can be induced by traces of Fe that were not completely removed from the original SWEOM samples.

The effect of various Fe-chelators on oogenesis was compared (Fig. 10). In the case of HBED and FC, which are known to be stronger chelators of Fe rather than EDTA, no mature gametophytes were observed. Although a few percent of maturities were observed in the presence of 1 μM Cat or PCA, no oogenesis was observed in the presence of 10 μM Cat or PCA. The stability constants for HEBD and FC are higher values ($\log K_{Fe(III)HBED}$ = 39.2, $\log K_{Fe(III)FC}$ = 28.5) than that for EDTA ($\log K_{Fe(III)EDTA}$ = 25). Dominant species of Fe in the presence of 10 μM Cat or PCA are simulated to stable 1:2 complexes (The β_2 values for $Fe(Cat)_2$ and $Fe(PCA)_2$ are 35 and 33, respectively), while the few percent of maturities observed in the presence of 1 μM Cat and PCA can be attributed to the minor distribution of 1:1 complexes, the stability constants ($\beta_{1\ Fe(III)Cat}$ = 20 and $\beta_{1\ Fe(III)PCA}$ = 19) are lower than that of EDTA(Iwai et al., 2015). Thus, Iwai et al. (2015) assumed that a labile complex species is favorable for oogenesis. In the case of 1 μM of EDTA, NTA, Cat or PCA added media,

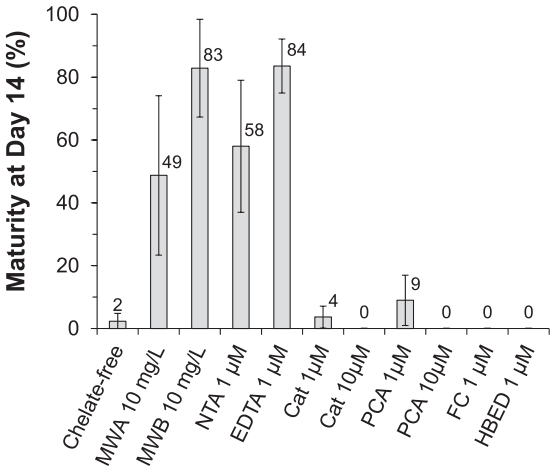

Figure 10. Percent maturity for a 14-day period for female gametophytes (*S. japonica*) in the ASP_{12} (Fe and EDTA-free) media adding various chelating agents and Fe (1 μM). Cat, PCA and FC mean catechol, protocatechuic acid, and ferrichrome, respectively. Values labeled on top of the columns and error bars represent average maturities (%) and standard deviations ($n = 3 - 5$), respectively. In the presence of various chelating agents (except for MWA and MWB), percent maturities in the absence of Fe were in the range of 0 – 2 %. The figure was referred from Iwai et al. (2015), *J. Appl. Phycol*., © Springer Science+Business Media 2015.

calculated concentrations of 1:1 Fe complexes was clearly correlated with the percent maturity, e.g., the ratios [Fe(III)L] (μM):maturity (%) for EDTA, NTA, Cat and PCA are 0.76:84, 0.50:58, 0.07:4 and 0.06:9, respectively (Iwai et al., 2015). In the case of 10 mg L^{-1} of SWEOM, the concentrations of complexed Fe were estimated to be lower values than that of EDTA, a large number of gametophytes could form eggs. Especially, the maturity for MWB was comparable with the value for EDTA (Fig. 10). Thus, it can be concluded that the SWEOM derived from a bark compost, especially MWB, is an effective DOM fraction for supplying favorable Fe species for support of stimulating gametogenesis.

Insights in algal Fe uptake mechanism

Even if the gametophytes cannot form eggs, they may take up Fe slowly (Nigi et al., 2000). It should be noted that the reproductive growth is a different response from the vegetative growth or iron accumulation reported in the large number of investigations (e.g., Hudson and Morel, 1990; Shaked et al., 2005; Morel et al., 2008; Salmon et al., 2006; Böttger et al., 2012), however, there is no doubt that iron is an essential nutrient for the reproductive growth in brown macroalgae (Motomura and Sakai, 1981). The mechanism of iron uptake in brown macroalgae is of fundamental to the reproductive growth.

The mechanisms responsible for iron uptake by terrestrial/higher plants are well understood to involve two basic strategies. Strategy I is an uptake mechanism involving ferrireductase and an Fe(II) transport protein (Moog and Bruggemann, 1994; Robinson et al., 1999). For example, the Strategy I plant cucumber (*Cucumis sativus L.*) was strong inhibited uptake of iron from Fe(III)HBED by ferrous complexing agent, bathophenanthroline disulfonic acid (BPDS) (Johnson et a., 2002). They suggested that the differences in ferric chelate reduction activity and Fe uptake are related to the activity of the ferrous transport system (Johnson et al., 2002). In the case of Strategy II plants, they secrete iron-specific binding compounds, such as a siderophore, and take up the Fe-siderophore complexes directly (Römheld and Marschner, 1986; Schaider et al., 2006). It has been known that bacteria and green algae employ Strategy II, they secrete siderophore and can direct the uptake of iron-siderophore complexes (Maldonado and Price, 2001; Soria-Dengg and Horstmann, 1995). The iron uptake mechanism for phytoplankton has been extensively investigated (e.g., Anderson and Morel, 1982; Hudson and Morel, 1990; Shaked et al., 2005; Sunda and Huntsman, 1995; Chen and Wang, 2001). Some studies predicted that the phytoplankton (e.g., *Thalassiosira weissflogii and Chaetoceros sociale*) take up inorganic iron dissociated from the dissolved chelator (Hudson and Morel, 1990; Shaked et al., 2005; Morel et al., 2008; Kuma et al., 1999). However, there is little information on the iron uptake mechanism for brown macroalgae. Manley (1981) and Böttger et al (2012) demonstrated that Fe uptake for brown macroalgae was drastically inhibited by the strong ferrous iron chelator, BPDS and FZ (Manley, 1981; Böttger et al., 2012). Matsunaga et al. (1991) investigated how to remove the adsorbed Fe on the cell surface of sporophytes. Their experiment showed that the chelating agents (EDTA and EDDHA) could not remove adsorbed Fe, however, the reducing agents (ascorbic acid and hydroxylaine) could remove all of the adsorbed Fe.

From this result, it can be considered that brown macroalgae have a specific Fe(III) binding site on their cell surface. Salmon et al. (2006) suggested that a FeL model in which Fe(III)DOM complexes are reduced to Fe(II)DOM complexes by a reductase on the cell membrane, and exchangeable Fe(II)DOM complexes or dissociated Fe(II) is taken up by binding to a ferrous transporter (Salmon et al., 2006). Recently, the entire genome of brown macroalga *Ectocarpus siliculosus*, which is a close relative kelp species, has been sequenced (Cock et al., 2010), and, Böttger et al. (2012) and Miller et al. (2014) investigated the iron uptake mechanism for *E. siliculosus* (Böttger et al., 2012; Miller et al., 2014). From the genomic data, *E. siliculosus* employed Strategy I because homologues of *fro2*, which is a proposed cell surface Fe(III) reductase, were identified in *E. siliculosus* (Cock et al., 2010; Böttger et al., 2012). Moreover, Miller et al. (2014) revealed that the binding of ferric iron to the cell surface is a critical step in iron uptake strategy of *E. siliculosus* (Miller et al., 2014). From these investigations, it can be proposed that the mechanism of iron uptake for brown macroalgae involves two steps, the binding ferric iron on the cell wall and the reduction of iron for uptake.

Nigi et al. (2000) reported that, FA (1 mg-C L^{-1}) significantly increased the values of iron uptake rate and adsorbed iron on sporophyte of *L. religiosa*, compared to those in the case of EDTA and ferric hydroxides (Nigi et al., 2000). In the restoration technique using an Fe-fertilizer, the concentration of iron eluted from the Fe-fertilizer will gradually decreases or diffuse to below 50 nM (Yamamoto et al., 2010a; Yamamoto et al., 2012), however, it can be expected that the iron bioavailability is enhanced by DOM derived from a compost, such as SWEOM. This may be one of the reasons for why seaweed restoration by means of the Fe-fertilizer succeeds for more than three years.

References

Abraham, E.R. (2007) Sea-urchin feeding frots. *Ecol. Complex*. **4**, 161-168.

Anderson, M.A. and Morel, F.M.M. (1982) The influence of aqueous iron chemistry on the uptake of iron by the coastal diatom *Thalassiosira weissflogii. Limnol. Oceanogr*. **27**, 789-813..

Böttger, L.H., Miller, E.P., Anderson, C., Matzanke, B.F., Küpper, F.C. and Carrano, C.J. (2012) A typical iron storage in marine brown algae: a multidiscriplinary study of iron transport and storage in *Ectocarpus siliculosus. J. Exp. Bot*. **63**, 5763-5772.

Chung, I.K., Beardall, J., Methta, S., Sahoo, D. and Stijkovic, S. (2011) Using marine macroalgae for carbon sequestration: a critical appraisal. *J. Appl. Phycol*. **23**, 877-886.

Cock, J.M., Sterck, L., Rouzé, P., Scornet, D., Allen, A.E., Amoutzias, G., Anthouard, V., Artiguenave, F., Aury, J.M., Badger, J.H., Beszteri, B., Billiau, K., Bonnet, E., Bothwell, J.H., Bowler, C., Boyen, C., Brownlee, C., Carrano, C.J., Charrier, B., Cho, G.Y., Coelho, S.M., Collén, J., Corre, E., Silva, C.D., Delage, L., Delaroque, N., Dittami, S.M., Doulbeau, S., Elias, M., Farnham, G., Gachon, C.M.M., Gschloessl, B., Heesch, S., Jabbari, K., Jubin, C., Kawai, H., Kimura, K., Kloareg, B., Küpper, F.C., Lang, D., Bail, A.L., Leblanc, C., Lerouge, P., Lohr, M., Lopez, P.J., Martens, C., Maumus, F., Michel, G., Miranda-Saavedra, D., Morales, J., Moreau, H., Motomura, T., Nagasato, C., Napoli, C.A., Nelson, D.R., Nyvall-Collén, P., Peters, A.F., Pommier, C., Potin, P., Poulain, J., Quesneville, H., Read, B., Rensing, S.A., Ritter, A., Rousvoal, S., Samanta, M., Samson, G., Schroeder, D.C., Ségurens, B., Strittmatter, M., Tonon, T., Tregear, J.W., Valentin, K., Dassow, P.V., Yamagishi. T., Van de Peer, Y. and Wincker, P. (2010) The *Ectocarpus* genome and the independent evolution of multicellularity in brown algae. *Nature* **465**, 617-621.

Fujii, M., Imaoka, A., Yoshimura, C. and Waite, T.D. (2014) Effects of molecular composition of natural organic matter on ferric iron complexation at circumneutral pH. *Environ. Sci. Technol*. **48**, 4414-4424.

Fujisawa, N., Fukushima, M., Yamamoto, M., Iwai, H., Komai, T., Kawabe, Y., Liu, D. (2012) Structural alterations of humic acid fractions in a steel slag-compost fertilization. Analysis by pyrolysis/methylation-gas chromatography/mass spectrometry. *J. Anal. Appl. Pyrolysis* **95**, 126-133.

Fujisawa, N., Furubayashi, K., Fukushima, M., Yamamoto, M., Komai, T., Ootsuka, K. and Kawabe, Y. (2011) Evaluation of the iron(II)-binding abilities of humic acids by complexometric

titration using colorimetry with *ortho*-phenanthroline. *Humic Substances Res*. **8**, 1-6.

Fujita, D. (2010) Current status and problems of isoyake in Japan. *Bull. Fish. Res. Agen*. **32**, 33-42.

Fukushima, M. and Iwai, H. (2011) Characterization and binding of Fe(II) in organic matter in a fertilizer including steel slag and compost to supply soluble Fe(II) to barren ground in coastal areas. *J. Adv. Mar. Sci. Technol. Soc*. **17**, 1-8.

Fukushima, M. and Tastumi, K. (1999) Light acceleration of iron (III) reduction by humic acid in the aqueous solution. *Colloid Surf. A-Physicochem. Eng. Asp*. **155**, 249-258.

Fukushima, M., Kikuchi, A., Tatsumi, K. and Tanaka, F. (2006) Separation of fulvic acid from soil extracts based on iron-pair. *Anal. Sci*. **22**, 229-233.

Fukushima, M., Nakayasu, K., Tanaka, S. and Nakamura, H. (1995) Chromium(III) binding abilities of humic acids. *Anal. Chim. Acta*. **317**, 195-206.

Fukushima, M., Tanaka, S. and Taga, M. (1994) Effect of ionic strength on complexing equilibrium between Copper(II) and humic acid. *Intern. J. Environ. Anal. Chem*. **56**, 229-237.

Gallois, N., Templier, J. and Derenne, S. (2007) Pyrolysis-gas chromatography-mass spectrometry of the 20 protein amino acids in the presence of TMAH. *J. Anal. Appl. Pyrolysis* **80**, 216-230.

Gao, K. and McKinley, K.R. (1994) Use of macroalage for marine biomass production and CO_2 remediation: a review. *J. Appl. Phycol*. **6**, 45-60.

Chen, M. and Wang, W.X. (2001) Bioaviability of natural colloid-bound iron to marine phytoplankton: Influences of colloidal size and aging. *Limnol Oceanogr*. **46**, 1956-1967..

Graham, M.H. (2010) Comparisons between East-Asia isoyake and deforestation in global kelp systems. *Bull. Fish. Res. Agen*. **32**, 47-50.

He, X., Xi, B., Wei, Z., Guo, X., Li, M., An, D and Liu, H. (2011) Spectroscopic characterization of water extractable organic matter during composting of municipal solid waste. *Chemosphere* **82**, 541-548.

Hudson, R.J.M and Morel, F.M.M. (1990) Iron transport in marine phytoplankton: Kinetics of cellular and medium coordination reactions. *Limnol. Oceanogr*. **35**, 1002-1020.

Iwai, H., Fukushima, M. and Yamamoto, M. (2012) Binding characteristics and dissociation kinetics for iron(II) complexes with seawater extractable organic matter and humic substances in a compost. *Anal. Sci*. **28**, 819-821.

Iwai, H., Fukushima, M. and Yamamoto, M. (2013b) Determination of Fe(II) species complexed with seawater extractable organic matter under seawater conditions based on the kinetics of ligand-exchange reactions with ferrozine. *Anal. Sci*. **29**, 723-728.

Iwai, H., Fukushima, M., Motomura, T., Kato, T. and Kosugi, C. (2015) Effect of iron complexes with seawater extractable organic matter on oogenesis in gametophytes of a brown macroalga (*Saccharina japonica*). *J. Appl. Phycol*. **27**, 1583-1591.

Iwai, H., Fukushima, M., Yamamoto, M., Komai, T. and Kawabe, Y. (2013a) Characterization of seawater extractable organic matter from bark compost by TMAH-py-GC/MS. *J. Anal. Appl. Pyrolysis* **99**, 9-15.

Johnson, G.V., Lopez, A. and La Valle Foster, N. (2002) Reduction and transport of Fe from siderophores. *Plant. Soil*. **241**, 27-33.

Kuma, K., Tanaka, J. and Matsunaga, K. (1999) Effect of natural and synthetic organic-Fe(III) complexes in an estuarine mixing model on iron uptake and growth of a coastal marine diatom, *Chaetoceros sociale. Mar. Biol*. **134**, 761-769.

Laglera, L.M. and van den Berg, C.M.G. (2009) Evidence for geochemical control of iron by humic substances in seawater. *Limnol. Oceanogr*. **54**, 610-619.

Lobban, C.S., and Harrison, P.J. (2000) In: *Seaweed ecology and phycoligy*. Cambridge. Cambridge, pp. 32-37.

Lv, B., Xing, M., Yang, J., Qi, W. and Lu, Y. (2013) Chemical and spectroscopic characterization of water extractable organic matter during vermicomposting of cattle dung. *Bioresour. Technol*. **132**, 320-326.

Lüning, K. and Neushul, M. (1978) Light and temperature demands for growth and reproduction of laminarialean gametophytes in southern and central California. *Mar. Biol*. **45**, 297-309.

Lüning, K. (1981) Egg release in gametophytes of *Laminaria Saccharina*: induction by darkness and inhibition by blue light and U.V. *Br. Phycol. J*. **16**, 379-393.

Macrellis, M.M., Trick, C.G., Rue, E.L., Smith, G. and Bruland, K.W. (2001) Collection and detection of natural iron-binding ligands from seawater. *Mar. Chem.* **76**, 175-187.

Maldonado, M.T. and Price, N.M. (2001) Reduction and transport of organically bound iron by *Thalassiosira oceanica* (Bacillariophyceae). *J. Phycol.* **37**, 298-309.

Manely, S.M. and North, W.J. (1981) In: *Proceedings of the 10th International Seaweed Symposium*. Pergamon. New York, pp467-472.

Manley, S.L. (1981) Iron uptake and translocation by *Macrocystis pyrifera. Plant. Physiol.* **68**, 914-918.

Mathuthu A.S. and Ephraim, J.H. (1993) Calcium binding by fulvic acids studied by an ion selective electrode and an ultrafiltration method. *Talanta* **40**, 521-526.

Matsunaga, K., Suzuki, Y. and Kuma, K. (1991) Uptake rate of iron by macroalgae from the Sea of Japan (*Laminaria religiosa* Miyabe and *Undaria pinnatifida*). *Bull. Japan. Soc. Fish. Oceanogr.* **55**, 349-353.

Matsunaga, K., Kawaguchi, T., Suzuki, Y. and Nigi, G. (1999) The role of terrestrial humic substances on the shift of kelp community to crustose coralline algae community of the Southern Hokkaido Island in the Japan Sea. *J. Exp. Mar. Biol. Ecol.* **241**, 193-205.

Matsunaga, K., Suzuki, Y., Kuma, K. and Kudo, I. (1994) Diffusion of Fe(II) from an iron propagation cage and its effect on tissue iron and pigments of macroalgae on the cage. *J. Appl. Phycol.* **6**, 397-403.

Millar, A.K. (2003) In: *Proceedings of the 17th International Seaweed Symposium,* Chapmann, A.R.O., Anderson, R.J., Vreeland, V.J., Davison, I.R., Eds.; Oxford University Press. Oxford, pp. 313-318.

Miller, E.P., Böttger, L.H., Weerasinghe, A.J., Crumbliss, A.L., Matznke, B.F., Meyer-Klaucke, W., Küpper, F.C., Carrano, C.J. (2014) Surface-bound iron: a metal ion buffer in the marine brown alga *Ectocarpus siliculosus*? *J. Exp. Bot.* **65**, 585-594.

Moog, P.R. and Bruggemann, W. (1994) Iron reductase systems on the plant plasama-membrane – a review. *Plant. Soil.* **165**, 241-260.

Morel, F.M.M., Kustka, A.B. and Shaked, Y. (2008) The role of unchelated Fe in the iron nutrition of phytoplankton. *Limnol. Oceanogr.* **53**, 400-404.

Motomura, T. and Sakai, Y. (1981) Effect of chelated iron in culture media on oogenesis in *Laminaria angustata. Bull. Jpn. Soc. Sci. Fish.* **47**, 1535-1540.

Motomura, T. and Sakai, Y. (1984) Regulation of gametogenesis of *Laminaria* and *Desmarestia* (Pheaophyta) by iron and boron. *Jpn. J. Phycol.* **32**, 209-215.

Nigi, G., Kuma, K. and Matsunaga, K. (2000) Effect of natural organic-Fe(III) complex iron uptake and growth of a brown alga *Laminaria religiosa* Miyabe. *Fish, Sci.* **66**, 986-988.

Nishimoto, R., Fukuchi, S., Qi, G., Fukushima, M., Sato, T. (2013) Effects of surface Fe(III) oxides in a steel slag on the formation of humic-like dark-colored polymers by the polycondensation of humic precursors. *Colloid Surf. A-Physicochem. Eng. Asp.* **418**, 117-123.

Paskins-Hurlburt, A.J., Skoryna, S.C., Tanaka, Y., Moore, W. and Stara, J.F. (1978) Fucoidan. Its binding of lead and other metals. *Bot. Mar.* **21**, 13-22.

Perdue, E.M., Beck, K.C. and Reuter, J.H. (1976) Organic complexes of iron and aluminum in natural waters. *Nature* **260**, 418-420.

Perreault, M.C., Borgeaud, I.A. and Gaymer, C.F. (2014) Impact of grazing by the sea urchin *Tetrapygus niger* on the kelp *Lessonia trabeculata* in Northern Chile. *J. Exp. Mar. Biol. Ecol.* **453**, 22-27.

Pham, A. N., Rose, A. L., Feitz, A. J. and Waite, T. D. (2006) Kinetics of Fe(III) precipitation in aqueous solutions at pH 6.0–9.5 and 25 °C. *Geochim. Cosmochim. Acta.* **70**, 640-650.

Provasoli, L. (1963) In: *Proceedings of the 4th International Seaweed Synposium*. Pergamon. New York, pp.9-17.

Robinson, N.J., Procter, C.M., Connolly, E.L. and Guerinot, M.L. (1999) A ferric-chelate reductase for iron uptake from soils. *Nature* **397**, 694-697.

Rosen, M.J. (1978) In: *Surfactants and Interfacial Phenomena*. John Wiley & Sons. New York, pp. 104-105.

Römheld, V. and Marschner, H. (1986) Evidence for a specific uptake system for iron phytosiderophore in roots of grasses. *Plant. Physiol* **80**, 175-180.

Said-Pullicino, D., Kaiser, K., Guggenberger, G. and Gigliotti, G. (2007) Changes in the chemical composition of water-extractable organic matter

during composting: Distribution between stable and labile organic matter pools. *Chemosphere* **66**, 2166-2176.

Salmon, T.P., Rose A.L., Neilan, B.A. and Waite, T.D. (2006) The FeL model of iron acquisition: Nondissociative reduction of ferric complexes in the marine environment. *Limnol. Oceanogr*. **51**, 1744-1754.

Schaider, L.A., Parker, D.R. and Sedlak, D.L. (2006) Uptake od EDTA-complexed Pb, Cd and Fe by solution and sand-cultured *brassica juncea. Plant. Soil*. **286**, 377-391.

Shaked, Y., Kustka, A.B. and Morel, F.M.M. (2005) A general kinetic model for iron acquisition by eukaryotic phytoplankton. *Limnol. Oceanogr*. **50**, 872-882.

Silverstein, R.M. and Webster, F.X. (1998) In; *Spectrometric Identification of Organic Compounds*. John Wiley & Sons. New York, pp. 81-109.

Soria-Dengg, S. and Horstmann, U. (1995) Ferrioxamines B and E as iron source for the marine diatom *Phaeodactylum tricornutum. Mar. Ecol. Prog. Ser*. **127**, 269-277.

Sunda, W.G. and Huntsman, S.A. (1995) Iron uptake and growth limitation in oceanic and coastal phytoplankton. *Mar. Chem*. **50**, 189-206.

Suzuki, Y. Kuma, K. and Matsunaga, K. (1994) Effect of iron on oogonium formation, growth rate and pigment synthesis of *Laminaria japonica* (pheaophyta). *Fish. Sci*. **60**, 373-378.

Suzuki, Y., Kuma, K. and Matsunaga, K. (1995) Bioavailability iron species in seawater measured by macroalga (*Laminaria japonica*) uptake. *Mar. Biol*. **123**, 173-178.

Swift. R.S. (1996) In: *Methods of Soil Analysis: Part 3 – Chemical Methods*, Spark, D.L., Eds; Soil Science Society of America Inc. Wisconsin, pp. 1018-1020.

Tan, K.H. (2003a) In: *Humic matter in soil and the environment. Principles and controversies*. Marcel Dekker, Inc. New York, pp. 23-25.

Tan, K.H. (2003b) In: *Humic matter in soil and the environment. Principles and controversies*. Marcel Dekker, Inc. New York, pp. 45-49.

Tegner, M.J. and Dayton, P.K. (1991) Sea urchins, El Niños, and the long term stability of Southern California kelp forest communities. *Mar. Ecol. Prog. Ser*. **77**, 49-63.

Tipping, E. (2002a) In: *Cation binding by humic substances*. Cambridge University Press. Cambridge, pp. 157-169.

Tipping, E. (2002b) In: *Cation binding by humic substances*. Cambridge University Press. Cambridge, pp. 288-333.

Tipping, E. (2002c) In: *Cation binding by humic substances*. Cambridge University Press. Cambridge, pp. 262-287.

Tipping, E. (2002d) In: *Cation binding by humic substances*. Cambridge University Press. Cambridge, pp. 4-11.

Warshaw, R.L., Kennedy, K.R. and Henrich, J.E. (1998) In: *Humic Substances: Structures, Properties and Uses*, Davies, G. and Ghabbour, E.A., Eds; The Royal Society of Chemistry. Cambridge, pp. 29-46.

Yamamoto, M., Fukushima, M. and Liu, D. (2012) The effect of humic substances on iron elution in the method of restoration of seaweed beds using steelmaking slag. *ISIJ Int*. **52**, 1909-1913.

Yamamoto, M., Fukushima, M., Kiso, E., Kato, T., Shibuya, M. Otsuka, K., Nishida, A. and Komai, T. (2010a) Application of iron-humates to a coastal areas of barren ground for restoring seaweed bed. *J. Chem. Eng. Jpn*. **43**, 627-634.

Yamamoto, M., Nishida, A., Otsuka, K., Komai, T. and Fukushima, M. (2010b) Evaluation of binding or iron (II) to humic substances derive from a compost sample by a colorimetric method using ferrozine. *Bioresource. Technol*. **101**, 4456-4460.

Ytreberg, E., Karlsson, J., Hoppe, S., Eklund, B. and Ndungu, K. (2011) Effect of organic complexation on copper accumulation and toxicity to the estuarine red macroalga *Ceramium tenuicorne*: A test of the free ion activity model. *Environ. Sci. Technol*. **45**, 3145-3153.